



# ACOUSTICS 2012

## Sound absorption by perforated walls with bias / grazing flow: experimental study of the influence of perforation angle

E. M.T. Moers<sup>a</sup>, D. Tonon<sup>b</sup> and A. Hirschberg<sup>b</sup>

<sup>a</sup>Dynamics and Control group, Department of Mechanical Engineering, Eindhoven University of Technology, P.O.B. 513, 5600 MB Eindhoven, Netherlands

<sup>b</sup>Mesoscopic Transport Phenomena, Department of Applied Physics, Eindhoven University of Technology, P.O.B. 513, 5600 MB Eindhoven, Netherlands

e.m.t.moers@tue.nl

Perforated walls are commonly used in acoustical dampers. In combustion chambers the liners are obliquely perforated. This allows a bias flow to provide film-cooling for protecting the wall. Perforated liners with bias flow result in significant sound absorption, which is favorable for flame stability.

We present experimental data on the effect of bias/grazing flow in the Strouhal number range of order unity or lower for three perforation angles ( $30^\circ$ ,  $90^\circ$  and  $150^\circ$ ) with respect to the wall.

Oblique perforations have a sharp edge which result into an improved sound absorption compared to orthogonal perforations. As a result the obliquely perforated walls display less potential for whistling when the bias flow velocity is of the same order as the grazing flow velocity.

## 1 Introduction

Film-cooling is widely applied to protect the walls of combustion chambers. Cool air is blown into the chamber by oblique perforations of the liners. Jet flows are formed at each perforation. Due to the Coanda effect, the flow remain attached to the wall and the film of cool air protects the walls of the engines from the hot combustion gas [5]. Another problem arising in combustion systems are thermoacoustic instabilities due to unsteady heat release. Acoustic damping can be used to limit pulsation amplitudes or even prevent self-sustained oscillations. It is known from Bechert [2] that sound absorption at perforations subjected to bias flow prevail at low Strouhal numbers ( $St \ll 1$ ). However for manufacturing reasons the use of large perforations is advantageous. Therefore the acoustic absorption behavior at higher Strouhal numbers is important.

In order to design liner structures with oblique perforations as thermal shield and as acoustic damper, it is necessary to understand the sound absorption at the oblique perforations in the presence of a combined bias and grazing flow. Hersch and Rogers [6], Baumeister and Rice [1] and Sun et al. [11] studied the absorption for orthogonal wall perforations subjected to a combination of bias and grazing flow at low Strouhal numbers. Recently, Lahiri et al. [10] investigated the effect of several geometrical parameters on the damping performance of perforated liners subjected to a bias flow. Apart from the numerical investigation by Eldredge et al. [5] on the behavior of oblique perforations in bias/grazing flows, we have little information about the effect of the perforation angle on the acoustical absorption.

In the present paper we describe an experimental study of the effect of perforation angle  $\theta$  and bias/grazing flow, on the acoustical absorption by wall perforations for Strouhal numbers of order unity.

## 2 Experimental setup

### 2.1 Instrumentation

Measurements are performed in a semi-anechoic room with a cut-off frequency of 300 Hz. An overview of the setup is shown in Figure 1. A 700 mm long smooth cylindrical tube with an inner radius of  $R = 35$  mm and 20 mm wall thickness is used as impedance tube. Seven piezoelectric dynamic pressure sensors (*PCB 116A*) are flush-mounted at the inner wall of the impedance tube. Each microphone is connected to a charge amplifier (*Kistler 5011*). An harmonic signal from a signal generator is sent through an amplifier to the loudspeaker. The signals from the charge amplifiers of the microphones as well as the signal from the signal generator are sampled simultaneously by an 8 channel DSA card at a sample rate of 10490 Sa/s. More details concerning above

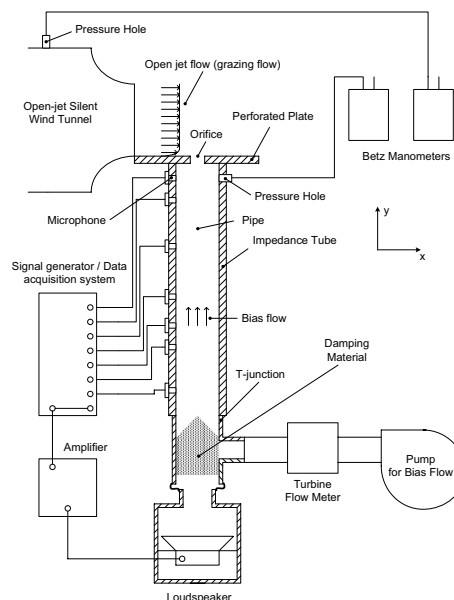


Figure 1: Schematic layout of the impedance tube setup.

mentioned instrumentation can be found in [9, 13].

Perforation test plates are mounted on the front end of the tube and are fixed to the nozzle (with  $0.2\text{ m} \times 0.2\text{ m}$  cross section) of a silent open jet wind tunnel, which provides the grazing flow along the perforation. A turbulent boundary layer is forced by using a 30 mm broad strip of sandpaper at the exit of the nozzle of the wind tunnel. The grazing flow velocity is  $u_g = 16.8\text{ m/s}$  and is determined by means of a pressure measurement. A silent organ pump (*Ventola GmbH & Co type 3/80*) is connected to the impedance tube to provide the bias flow through the perforation. A turbine gas meter (*Dresser IMTM-CT G65 DIN PN16 DN50*) is mounted between the pump and the impedance tube to measure the bias volume flow rate  $\Phi_b$ . The static pressure  $\Delta p_j$  in the impedance tube relative to the atmospheric pressure is measured at a pressure hole in the wall of the impedance tube with a Betz manometer (*Nonius Delft*) within an accuracy of 2 Pa. The pressure hole is positioned 20 mm from the front end of the impedance tube. In a similar manner the difference  $\Delta p_0$  between the static pressure in the settling chamber of the wind tunnel and the static pressure in the jet is measured within an accuracy of 1 Pa. Therefore we have  $u_g = \sqrt{2\Delta p_0/\rho_0}$  with  $\rho_0 = 1.2\text{ kg/m}^3$ . The temperature of the air is measured with an accuracy of  $0.1^\circ\text{ C}$  by means of a digital thermometer (*Omega HH309A*).

Measurement results are shown for frequencies between 63 Hz and 869 Hz. For each measured frequency, the microphone signals are recorded over a period of 3 s. The time signal of the microphones and the reference signal from the

signal generator are post-processed using a lock-in method and a multi-microphone method [9]. Tests with a closed wall indicate an accuracy in the measured reflection coefficient of 1% for the considered frequency range.

## 2.2 Perforation geometries and flow direction

In this paper we consider three single slit-shaped perforations of width  $w$  in plates of thickness  $t = 15$  mm with different angle of inclination  $\theta = 150^\circ$ ,  $90^\circ$  and  $30^\circ$ . Figure 2 shows a cross section of the perforated plates. The plate is attached with one side on the end of the impedance tube, the other side is subjected to the grazing flow. The edges of the perforation are sharp. The length of the long edge of each slit shaped perforations is  $h = 50$  mm. This edge is perpendicular to the grazing flow direction. The perforation length is  $t/\sin\theta$ .

The distance from the wind tunnel nozzle exit to the upstream edge of the perforation is  $L_w$ . The direction of the bias outflow (positive value of  $u_b$ ) and grazing flow are shown by the arrows in Figure 2. Bias inflow is directed in opposite bias flow direction (negative  $u_b$ ). The magnitude of the bias velocity  $u_b$  is the flow velocity averaged over the perforation cross section  $S_h$ :  $u_b = \Phi_b/S_h$  with  $\Phi_b$  the bias volume flow rate and  $S_h = hw \sin\theta$ .

## 2.3 Acoustic perforation resistance

According to Kooijman et al. [9], the one-sided perforation impedance  $Z_{h,in}$  is for an harmonic signal:

$$Z_{h,in} = \frac{1}{\rho_0 c_0} \frac{p_{in}}{u_h} \quad (1)$$

where  $p_{in}$  is the complex amplitude of the acoustic pressure at the inner side of the perforation (in the impedance tube) and  $u_h$  is the complex amplitude of the acoustic velocity through the perforation. In order to focus on the contribution of the flow at the perforation, we subtract the perforation impedance in the absence of flow  $Z_{h,in,u=0}$  from the perforation impedance with flow  $Z_{h,in}$  [9]. We scale this by the Mach number based on the grazing flow velocity  $M_g = u_g/c_0$  with  $c_0$  the speed of sound. The sound absorption is determined by the acoustic perforation resistance  $r_g$ ; the real part of the one-sided scaled acoustic perforation impedance:

$$r_g = \frac{1}{M_g} \Re \{ Z_{h,in} - Z_{h,in,u=0} \} \quad (2)$$

which can be obtained experimentally by following the measurement and postprocessing procedure as it is briefly described in section 2.1. In this approach we assume that for a given acoustic flow through the perforation  $u_h$ , the acoustical pressure outside the perforation is not significantly affected by the grazing or bias flow. The scaled acoustic resistance  $r_g$  is measured for different flow configurations and Strouhal number based on the grazing velocity  $Sr_g$

$$Sr_g = \frac{fw}{u_g} \quad (3)$$

where  $f$  is the frequency. Similarly the Strouhal number based on the bias flow is:

$$Sr_b = \frac{ft}{|u_b| \sin\theta} \quad (4)$$

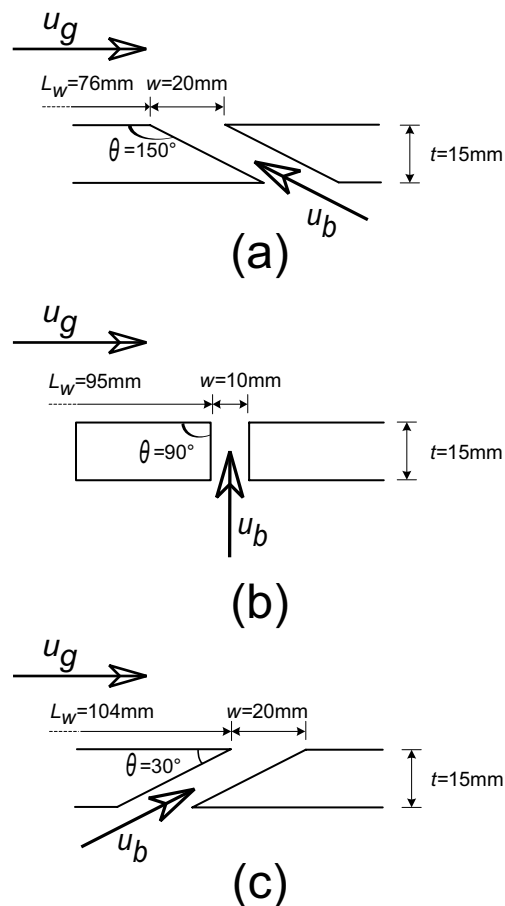


Figure 2: Schematic presentation of the three perforations: (a) perforation oblique in grazing flow direction ( $\theta = 150^\circ$ ), (b) perforation with orthogonal edges ( $\theta = 90^\circ$ ) and (c) perforation oblique in opposite grazing flow direction ( $\theta = 30^\circ$ ). The arrow with subscript  $u_g$  indicate the grazing flow direction, the arrow with subscript  $u_b$  the bias outflow direction. Bias inflow is directed opposite to the bias outflow.

## 3 Experimental results

### 3.1 Pure grazing flow

In Figure 3 the measured acoustic perforation resistance  $r_g$  is shown as a function of the Strouhal number  $Sr_g$  for a grazing flow velocity  $u_g = 16.8$  m/s and a turbulent boundary layer upstream of the perforation. The perforations have different angle of inclination with respect to the grazing flow direction;  $\theta = 150^\circ$ ,  $\theta = 90^\circ$  and  $\theta = 30^\circ$ .

For the perforations with  $\theta = 150^\circ$  and  $\theta = 90^\circ$ , peaks of sound absorption ( $r_g > 0$ ) and amplification ( $r_g < 0$ ) are observed at critical Strouhal numbers which corresponds with the hydrodynamic modes of the shear layer over the perforation opening [9, 3, 4, 8].

For the perforation with  $\theta = 30^\circ$ , sharp upstream edge, no peaks of sound amplification are observed. Only a reduced value of the resistance  $r_g$  is found for Strouhal numbers around 0.65.

At low Strouhal numbers  $0.05 \leq Sr_g \leq 0.30$ , it is remarkable that the perforation with  $\theta = 150^\circ$  has a negative acoustic resistance.

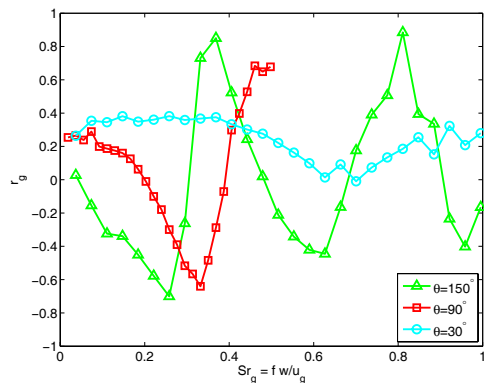


Figure 3: Pure grazing flow: acoustic perforation resistance  $r_g$  for the perforations with an obtuse upstream angle ( $\theta = 150^\circ$ ), orthogonal edges ( $\theta = 90^\circ$ ) and an acute upstream angle ( $\theta = 30^\circ$ ). The grazing flow velocity is  $u_g = 16.8$  m/s outside the boundary layer.

### 3.2 Combined grazing and bias inflow

For comparison to the pure grazing flow case with  $u_g = 16.8$  m/s, a bias inflow is added so that the ratio of velocity magnitudes is  $u_b/u_g = O(-1)$ . The same scalings are used for  $r_g$  and  $Sr_g$  as for a pure grazing flow. The results are shown in Figure 4.

For all three perforations having different angle of inclination, the addition of a bias inflow increases the acoustic resistance up to Strouhal numbers of order unity. Since  $|u_b|/u_g = O(1)$ , the effect of the formation of a jet due to flow separation will increase the sound absorption, similar as for a pure bias flow case. This behavior is well documented in literature [12, 8, 7]

At low Strouhal numbers, each perforation has a different acoustic resistance with grazing/bias inflow. In contrast with this, for a pure grazing flow the perforations with  $\theta = 90^\circ$  and  $\theta = 30^\circ$  showed similar resistance at low Strouhal numbers. Note that, depending on the ratio of  $|u_b|/u_g$ , we observed for the different perforations different values of the Vena Contracta ratio  $\Gamma = S_j/S_h$  with  $S_j$  the minimal cross sectional area of the jet. The values are:  $\Gamma = 0.8$  for  $\theta = 150^\circ$ ,  $\Gamma = 0.5$  for  $\theta = 90^\circ$  and  $\Gamma = 0.4$  for  $\theta = 30^\circ$ .  $\Gamma$  is estimated by calculating the jet velocity  $u_j = \sqrt{2\Delta p_j/\rho_0}$  from the measured static jet pressure  $\Delta p_j$  (see Figure 1) and the measured bias volume flow  $\Phi_b$ . Using the formula for the bias flow  $u_b$  in section 2.2, we obtain  $\Gamma = \Phi_b/(wh \sin \theta u_j)$ .

The largest absorption with  $r_g \approx 4$  is observed for  $\theta = 90^\circ$  around  $Sr_g = 0.4$ . However, around  $Sr_g = 0.25$ , the resistance  $r_g$  almost vanishes. This dip in the absorption is expected to be related to the whistling behavior observed for perforations subjected to a pure bias flow around  $Sr_b = 0.36$  [12].

The constant absorption with magnitude  $r_g = O(1)$  as observed for the perforation with  $\theta = 150^\circ$  can be an advantage if sound absorption over a larger frequency band is desired. For  $\theta = 30^\circ$  a large absorption is observed up to  $Sr_g = 1$ .

### 3.3 Combined grazing and bias outflow

Figure 5 shows the results for a combination of grazing flow and bias outflow with  $u_b/u_g = O(1)$ . Compared to pure grazing flow, the application of a strong bias outflow increases the sound absorption.

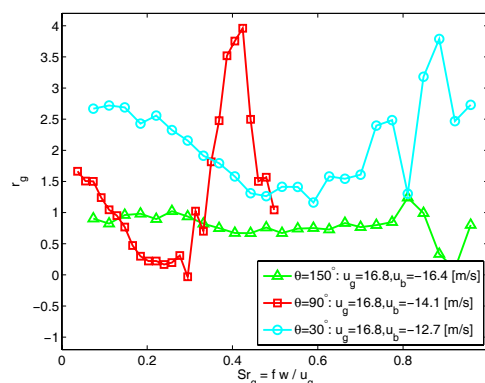


Figure 4: Grazing/bias inflow: acoustic perforation resistance  $r_g$  for the perforations having different angle of perforation:  $\theta = 150^\circ$  with  $|u_b|/u_g = 0.98$ ,  $\theta = 90^\circ$  with  $|u_b|/u_g = 0.84$  and  $\theta = 30^\circ$  with  $|u_b|/u_g = 0.76$ .

For outflow, at low Strouhal numbers and for  $\theta = 150^\circ$ ,  $r_g$  is of the same order ( $r_g \approx 2.5$ ) as the low Strouhal number resistance for  $\theta = 30^\circ$  and inflow. We expect that for these configurations the effect of flow separation and bending of the steady flow at the sharp edge of the perforation has a strong impact on the acoustic resistance.

For  $\theta = 90^\circ$  oscillations in  $r_g$  as a function of  $Sr_g$  are much more pronounced than for the oblique perforations. The potential of whistling due to the bias flow is observed at critical Strouhal numbers  $Sr_b = 0.2$  and  $0.5$ . Similar behavior was observed for grazing/bias inflow (see section 3.2).

Around  $Sr_g = 0.8$ , for  $\theta = 150^\circ$ , large acoustic dissipation occurs with  $r_g \approx 6$ .

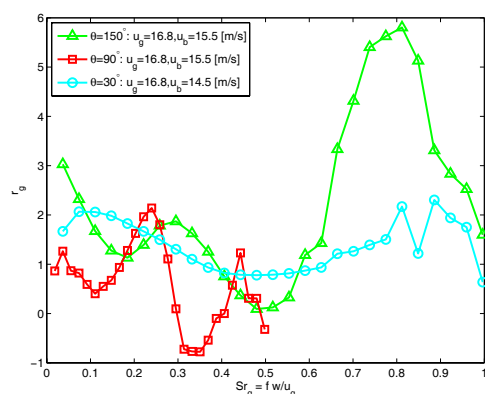


Figure 5: Grazing/bias outflow: dimensionless scaled acoustic resistance  $r_g$  for the perforations having different angle of perforation:  $\theta = 150^\circ$  with  $|u_b|/u_g = 0.98$ ,  $\theta = 90^\circ$  with  $|u_b|/u_g = 0.84$  and  $\theta = 30^\circ$  with  $|u_b|/u_g = 0.76$ .

## 4 Conclusion

We have obtained accurate measurements of the effect of grazing and bias flow on the linear acoustic response of wall perforations with sharp edges at low Mach numbers. We have presented the real part of the dimensionless impedance, which is relevant for acoustical damping. In particular we compare the behavior of oblique perforations (angles  $\theta = 30^\circ$  and  $\theta = 150^\circ$ ) with that of normal perforations ( $\theta = 90^\circ$ ).

For pure grazing flow, the response displays minima in the acoustical resistance  $r_g$  at critical Strouhal numbers  $Sr_g = fw/u_g$  based on the opening width in flow direction  $w$ . In some cases a negative resistance is found, which corresponds to potential whistling. The depth of this minima correlates with the shape of the geometry of the upstream edge of the perforation on the grazing flow side. A sharp upstream edge ( $\theta = 30^\circ$ ) will prevent whistling. This effect of the upstream edge corresponds to the effect reported in earlier studies [3, 4, 9] and can be explained in terms of Vortex Sound Theory.

A strong bias flow  $|u_b|/u_g = O(1)$  will induce potential whistling for normal perforations ( $\theta = 90^\circ$ ) at critical Strouhal numbers  $Sr_b = ft/u_b$  based on the plate thickness  $t$  as observed for pure bias flow by Testud [12]. An oblique perforation ( $\theta = 30^\circ$  or  $\theta = 150^\circ$ ) significantly reduces this problem when  $|u_b|/u_g = O(1)$ .

Summarizing, perforated walls with bias/grazing flow will absorb sound at low Strouhal numbers. At higher Strouhal numbers (order unity) the flow can display self-sustained oscillation (whistling). A safe design to avoid self-noise implies therefore the use of small perforations. The potential whistling is however sensitive to both the geometry of the perforation and the ratio of bias/grazing flow. Our study indicates that oblique perforations with a sharp upstream edge at the grazing flow side ( $\theta = 30^\circ$ ) is a safe acoustical design. Bias flow will further reduce the potential for whistling in oblique perforations ( $\theta = 30^\circ$  or  $\theta = 150^\circ$ ), which is not the case for orthogonal perforations ( $\theta = 90^\circ$ ).

## References

- [1] K.J. Baumeister, E.J. Rice, "Visual study of the effect of grazing flow on the oscillatory flow in a resonator orifice", *Nasa Technical Memorandum*, **3288** (1973)
- [2] D.W. Bechert, "Sound absorption caused by vorticity shedding, demonstrated with a jet flow", *Journal of Sound and Vibration*, **70(3)**, 389-405 (1980)
- [3] J.C. Bruggeman, A. Hirschberg, M.E.H. van Dongen, A.P.J. Wijnands, J. Gorter, "Self-sustained aeroacoustic pulsations in gas transport systems: Experimental study of the influence of closed side branches", *Journal of Sound and Vibration*, **150(3)**, 371-393 (1991)
- [4] S. Dequand, X. Luo, J. Willems, A. Hirschberg, "Helmholtz-Like Resonator Self-Sustained Oscillations, Part 1: Acoustical Measurements and Analytical Models", *AIAA Journal*, **41(3)**, 408-415 (2003)
- [5] J.D. Eldredge, D.J. Bodony, M. Shoeybi, "Numerical investigation of the acoustic behavior of a multi-perforated liner", *13th AIAA/CEAS Aeroacoustics Conference*, **3683** (2007)
- [6] A.S. Hersch, T. Rogers, "The effect of grazing flow on the steady state resistance of square-edged orifices", *American Institute for Aeronautics and Astronautics*, **493** (1975)
- [7] G.C.J. Hofmans, M. Ranucci, G. Ajello, Y. Aurégan, A. Hirschberg, "Aeroacoustic response of a slit-shaped diaphragm in a pipe at low Helmholtz number, 2: unsteady results", *Journal of Sound and Vibration*, **244(1)**, 57-77 (2000)
- [8] M.S. Howe, "Acoustics of Fluid-Structure Interactions", *Cambridge University Press* (1998)
- [9] G. Kooijman, A. Hirschberg, J. Golliard, "Acoustical response of orifices under grazing flow: Effect of boundary layer profile and edge geometry", *Journal of Sound and Vibration*, **315**, 849-874 (2008)
- [10] C. Lahiri, L. Enghardt, F. Bake, S. Sadig, M. Gerendás, "Establishment of a high quality database for the acoustic modeling of perforated liners", *Journal of Engineering for Gas Turbines and Power*, **133**, 091503-1:9 (2011)
- [11] X. Sun, X. Jing, H. Zhang, Y. Shi, "Effect of grazing/bias flow interaction on acoustic impedance of perforated plates", *Journal of Sound and Vibration*, **254(3)**, 557-573 (2002)
- [12] P. Testud, Y. Aurégan, P. Moussou, A. Hirschberg, "The whistling potentially of an orifice in a confined flow using an energetic criterion", *Journal of Sound and Vibration*, **325**, 769-780 (2009)
- [13] D. Tonon, "Aeroacoustics of shear layers in internal flows: closed branches and wall perforation", PhD thesis, Eindhoven University of Technology (2011)